

Possibility of drug delivery due to hydrogen bonds formation in nanodiamonds and doxorubicin: molecular modeling

A. N. Bokarev, I. L. Plastun

Saratov State Technical University named after Yuri Gagarin, Saratov, Russia

andreybokarev@mail.ru, inna_pls@mail.ru

PACS 36.40.Mr

DOI 10.17586/2220-8054-2018-9-3-370-377

The possibility of drug delivery and retention in cells due to hydrogen bond formation between enriched nanodiamonds and highly toxic drugs (for example doxorubicin), is investigated by numerical simulation. Using molecular modeling by the density functional theory method with the B3LYP functional and the 6-31G(d) basic set, we analyze hydrogen bond formation and their influence on IR-spectra and structure of molecular complex which is formed due to interaction between doxorubicin and nanodiamonds enriched by carboxylic groups. Numerical modeling of carboxylated nanodiamonds and doxorubicin interaction is based on nanodiamond representation by a diamond-like nanoparticle with simpler structure. Enriched adamantane (1,3,5,7-adamantanetetracarboxylic acid) is used as an example of carboxylated diamond-like nanoparticle. Combined IR spectrum as imposing of IR spectra for doxorubicin and 1,3,5,7-adamantanetetracarboxylic acid various interaction positions is obtained. The combined IR spectrum demonstrates good agreement with experimental data. The obtained results demonstrate that there can be strong hydrogen bonds between doxorubicin and nanodiamond as one of basic mechanism for drug delivery and retention in cells.

Keywords: doxorubicin, nanodiamond, drug delivery, 1,3,5,7-adamantanetetracarboxylic acid, molecular complex, hydrogen bond, molecular modeling, density functional theory, IR spectrum.

Received: 23 December 2017

Revised: 15 March 2018

Final revision: 20 March 2018

1. Introduction

Detonation nanodiamond (ND) is one of most promising materials for targeted drug delivery [1–3] – one of rapidly developing areas of modern chemistry, pharmacology and medicine. Wide possibilities for surface modification and advantageous dimensions make nanodiamonds very attractive objects for use in the drug delivery process. Many experimental studies are devoted to increasing the efficiency of tumor treatment by using drugs in combination with nanodiamonds [4–12]. It is nontoxic, biocompatible and able to overcome biological barriers, penetrating into the cells [10]. For the immobilization of drugs on ND surface are commonly used an adsorption [11] and covalent grafting [8, 12] methods.

A number of studies have shown that therapeutic efficacy of drugs is enhanced and their toxicities may be attenuated with immobilization on ND. Such studies are: investigation of amikacin-immobilized ND antibacterial activity [8], enhance of drug retention in cancer cells due to ND-mitoxantrone molecular complexes [13], flavonoids transport due to diamond-like nanoparticles [14], enhance therapeutic efficacy of doxorubicin due to ND [9, 15] and many other studies (see, for example, reviews [4] and [6]).

As noted above, the most popular methods of drug immobilization on ND surface are adsorption and covalent grafting, but also there is one more simple immobilization method – creation of molecular complex due to hydrogen bond formation, that is due to electrostatic interaction. One of example for drug and ND electrostatic interaction analysis is doxorubicin (DOX) ($C_{27}H_{29}NO_{11}$). It is one of the most well-known and widely used drugs for the treatment of cancer. Unfortunately, DOX, like most anticancer drugs, is toxic. Doctors must limit the dose administered since doxorubicin can cause major side effects such as hair loss, nausea [16], and weakening of the heart muscle over time (cardiomyopathy) [17]. Significant reduction in side effects can be achieved by increasing the efficiency of the mechanism for drug delivery to tumor cells.

Theoretical investigation of DOX and ND electrostatic interaction and analysis of DOX–ND molecular dynamic depending on a pH-factor was conducted in [15], where in modeling process used a bare ND. However, in real nature experiments usually used an enriched ND, containing various functional groups as $-COOH$, $-CONH$, $-OH$, $-CO$, $-NH_2$, $-SH$, $-CH_2$, $-H$, etc. (see, for example, [6]). The enriched ND surface promotes strengthening of the intermolecular interactions that, as a result, causes increase in the drug delivery efficacy.

Experimental studies of DOX and enriched ND molecular complexes, formed as a result of electrostatic interaction, demonstrate a significant enhancement of DOX therapeutic efficacy [9]. In this article conclusion, it is

said that the effect of DOX enhancement is found, but the mechanism of its emergence is not explained. Theoretical studies of DOX and ND intermolecular interaction will be able to offer an explanation for this mechanism, but now investigation of DOX and ND electrostatic interaction and analysis of hydrogen bonds formation in DOX–ND molecular complex have not been carried out. For this reason, such study is quite relevant as attempt of an explanation of DOX efficacy enhancement mechanisms.

Thus, the aim of present work is investigation of hydrogen bond formation between DOX and COOH-enriched ND by analysis of calculated IR spectra and optimized structures of formed molecular complexes. ND are a means of drug retention in cancer cells. Energy of formed hydrogen bonds will define a use possibility for ND as tool of drug delivery and retention in cells due to electrostatic interaction mechanism.

2. Molecular modeling

Molecular modeling was executed by numerical simulation based on the density functional theory [18], in particular, on the B3LYP functional method [19]. In B3LYP method there is representation of the molecular orbital as a linear combination of linearly independent functions, which are called basis functions. For numerical simulations, we used split-valence basis sets. These sets are characterized by high accuracy, which is achieved by the valence orbital representation by two sets of functions. The notation for the split-valence basis sets is typically *M*-NPG, where *M* denotes the number of primitive Gaussian functions which are included in the basis function of atomic orbital (*M* takes values from 3 to 6), the *N* and *P* show that the valence orbital are composed of two basis functions each, the first one composed of a linear combination of *N* primitive Gaussian functions (*N* is typically equal to 2 or 3), the other composed of a linear combination of *P* primitive Gaussian functions. In present work we use the split-valence 6-31G(d) basis set. Obviously, the atomic orbital of the inner electron shell is approximated by six Gaussian functions. Orbital of the valence shell is described, respectively, three and one Gaussian functions. For numerical modeling of intermolecular interaction in molecular compound we used the Gaussian 09 program complex [20], which is traditionally applied for investigations in various areas of computational physics and chemistry and approved by the authors in [14] and other investigations.

Procedures of molecular modeling and spectra calculations require a large amount of computational resources and time depending on the structure complexity of molecules, which form the compound, and on the total number of atoms in the complex. The typical ND has diameter of ~ 4 to 40 nm [4,6] and includes more than 1000 atoms. Therefore, the modeling of real ND and DOX interaction at the level of studying the possibility of intermolecular bond formation is very difficult for personal computers. For this reason, the question arises concerning the possibility of using small size diamond-like nanoparticles, which would be similar to large size nanodiamonds in their characteristics and intermolecular interaction capabilities.

In the process of molecular modeling by numerical simulations, we used a model based on the simplest diamondoid, adamantane. Adamantane ($C_{10}H_{16}$) is the smallest diamond-like hydrocarbon particle. The spatial arrangement of carbon atoms in adamantane molecule is the same as in the diamond crystal. This structure is the basic “building” block for larger diamond-like structures [21]. In present work, we consider the modified adamantane, named 1,3,5,7-adamantantetracarboxylic acid (AdTCA) ($C_{14}H_{16}O_8$), which contains 4 carboxylic (–COOH) groups [22]. The modified structure is resulted from the substitution of 4 hydrogen atoms for carboxylic groups in original adamantane. To assess the possibility of using AdTCA as an object that approximates a large-size carboxylated ND, we also calculated IR spectra for 1 nm diameter ND ($C_{88}H_{64}O_8$) enriched by 4 carboxylic groups. The chemical structures of adamantane, AdTCA and 1 nm diameter ND are presented on Fig. 1.

In order to account for anharmonicity in intermolecular interactions, we used the following scaling factors for resulted vibrational modes: 0.9713 (range 0 – 1000 cm^{-1}); 0.9744 (range 1000 – 2000 cm^{-1}); 0.956 (range above 2000 cm^{-1}). These factors are used to decrease the divergence between calculated and experimental data, which is caused by using the harmonic approximation in numerical simulations.

3. Results and discussion

In our investigations, we based our work on experimental results obtained in [9]. In this work, the ND–DOX molecular complex was obtained using a novel adsorption technique developed with a pH 8.5 coupling buffer. Follow the experimental results [9], we consider a ND–DOX molecular complex in crystal phase. As is shown in our preliminary calculation results, all hydrogen bonds are present in an aqueous phase, but their energy becomes a little less than in a crystal phase, and their investigation is not a subject for research in this article.

The structure of DOX molecule and the calculated IR spectrum of DOX in comparison with the experimental IR spectrum of DOX, taken from work [9], are shown in Figs. 2a and 2b, respectively. Peaks in the high-frequency region of the calculated IR spectrum (1 – 5 on Fig. 2b) correspond to stretching vibrations of O–H bonds in DOX

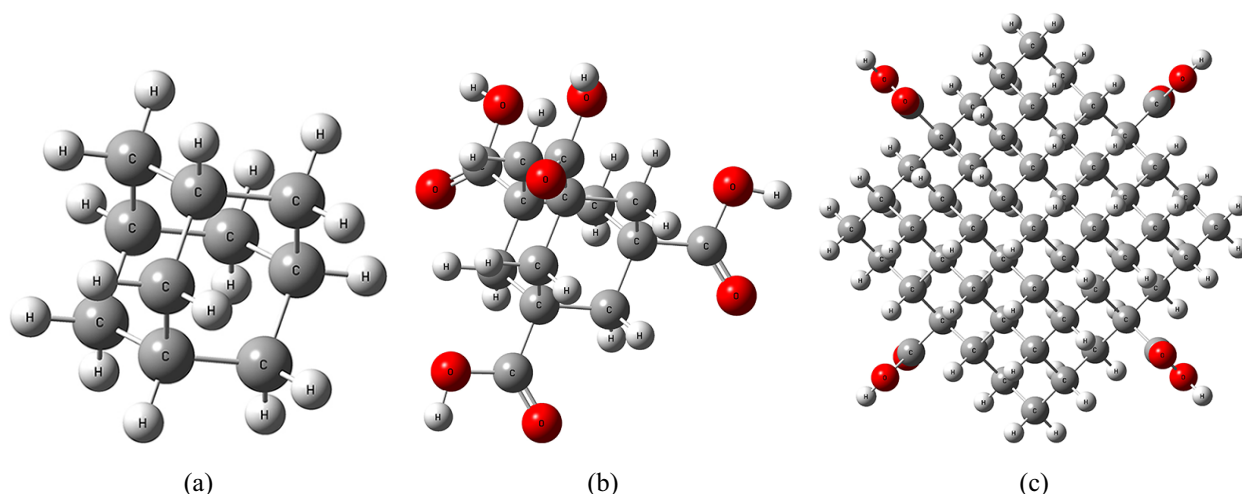


FIG. 1. Structure of adamantane (a), 1,3,5,7-adamantanetetracarboxylic acid $C_{14}H_{16}O_8$ (b) and 1 nm diameter nanodiamond $C_{88}H_{64}O_8$, enriched by 4 carboxylic ($-COOH$) groups (c)

(1 – 5 on Fig. 2a). After carrying out the frequencies scaling, the calculated spectrum is in good agreement with the experimental data.

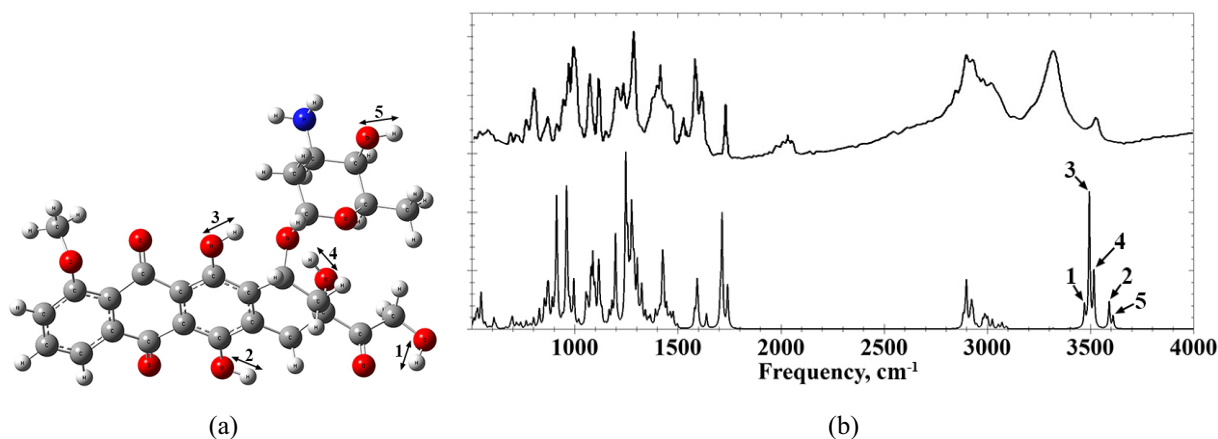


FIG. 2. Structure (a) and experimental (upper) and calculated (lower) IR spectra (b) of doxorubicin with designated 1–5 O–H bonds

The calculated frequencies of stretching vibrations for O–H bonds in DOX, which can participate in the formation of hydrogen bonds, are: 1 – 3472 cm^{-1} , 2 – 3591 cm^{-1} , 3 – 3495 cm^{-1} , 4 – 3517 cm^{-1} , 5 – 3610 cm^{-1} . The lengths of all O–H bonds are on the order of 0.97 \AA .

Let us consider the possibility of using AdTCA as an object that approximates a large-size carboxylated ND. In Fig. 3, we can compare calculated IR spectra of 1 nm diameter ND enriched by 4 $-COOH$ groups and AdTCA with experimental IR spectrum of carboxylated ND provided by the Laboratory of laser spectroscopy of solutions of supramolecular compounds and nanostructures (headed by T. A. Dolenko, Physics Department of Moscow State University).

In the calculated IR spectrum of AdTCA (Fig. 3, lower), there are four characteristic regions which correspond to stretching vibrations of C–O and C–C bonds ($1000 - 1200\text{ cm}^{-1}$), C=O bonds ($1780 - 1800\text{ cm}^{-1}$), C–H bonds ($2915 - 2995\text{ cm}^{-1}$) and stretching vibrations of O–H bonds (3523 cm^{-1}). The frequencies of the most intense peaks in the considered regions are 1144 cm^{-1} , 1795 cm^{-1} , 2917 cm^{-1} and 3523 cm^{-1} , respectively. The considered characteristic regions in the obtained IR spectra of AdTCA are in good agreement with the corresponding regions in the calculated IR spectrum of 1 nm diameter ND, enriched by 4 carboxylic groups (Fig. 3, center) and the experimental IR spectrum of carboxylated ND (Fig. 3, upper). However, the procedures of structure optimization and spectra calculations AdTCA require much less computational time than the calculation of 1 nm diameter ND.

Thus, the high level of consistency of the characteristic regions in considered spectra and a smaller amount of the required computational time allows the use of AdTCA as an object that approximates a large-size carboxylated ND at the level that allows qualitative estimation of compound formation during molecular modeling.

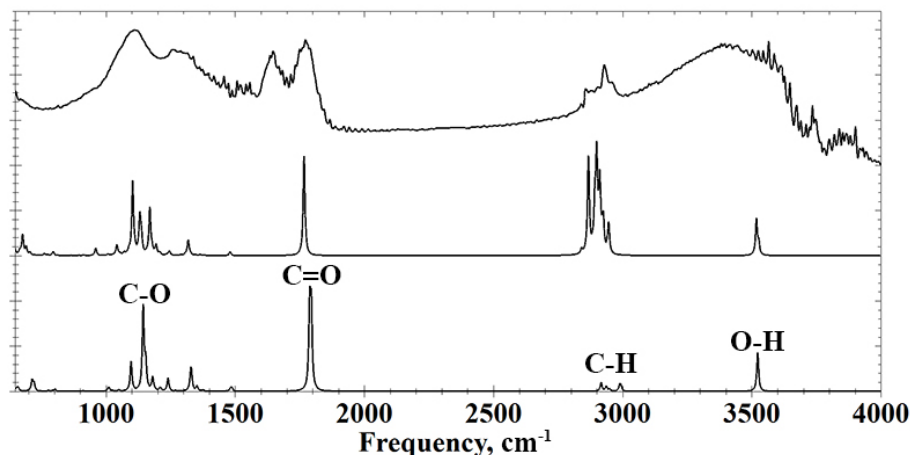


FIG. 3. Experimental IR spectrum of carboxylated nanodiamond (upper), calculated IR spectra of 1 nm diameter nanodiamond (central) and 1,3,5,7-adamantanetetracarboxylic acid (lower)

As we spoke above, the sizes of NDs, which are used in scientific experiments with DOX, are from 4 nm and higher [9], and the width of the DOX molecule is about 1.5 nm, therefore we can assume that the DOX molecule can be attached to the ND at several points simultaneously. The doxorubicin molecule includes five O–H bonds (1 – 5 on Fig. 2a) and two N–H bonds, whose hydrogen atoms can theoretically participate in the formation of hydrogen bonds as a donor, as well as eleven oxygen atoms and one nitrogen atom that can participate in the formation of hydrogen bonds as an acceptor. In our studies, we considered possible variants of interaction with all these atoms, but due to the limitations of molecular modeling caused by the structural features of AdTCA and ND and computation mechanism of energy optimization, only six variants of the complexes were obtained. Thus, in our calculations we investigate the parameters of hydrogen bonds, which are formed between AdTCA and DOX at all possible interaction positions. As a result of numerical simulation, we obtained optimized structures and the IR spectra of the six formed molecular complexes (Figs. 4 and 5) and analyzed the energy of intermolecular hydrogen bonds (H-bonds).

The energy of H-bonds is investigated by analysis of such parameters as length of a hydrogen bridge and the frequency shift. The energy of hydrogen bonds was estimated using empirical Iogansen formula [23]: $-\Delta H = 0.3(\Delta\nu - 40)^{1/2}$, where $\Delta\nu$ – frequency shift of the stretching vibration of O–H bond (ΔH in kcal/mol, $\Delta\nu$ – cm^{-1}).

According to the optimized structures and calculated IR spectra for six cases of molecular compound (Fig. 4 and Fig. 5), it can be noted that in all interaction positions the one H-bond or two H-bonds are formed between AdTCA and DOX.

Two peaks (1 and 2 in Fig. 4a and in Fig. 5c) at 3207 cm^{-1} and at 3376 cm^{-1} for case 1 (Fig. 4a) and for case 6 – at 3187 cm^{-1} and at 3362 cm^{-1} (Fig. 5c) correspond to stretching vibrations of O–H bond in AdTCA, which participates in the H-bond formation with DOX, and in DOX, which participates in the H-bond formation with AdTCA, respectively. In case 2, there are two formed intermolecular H-bonds between AdTCA and DOX which participate in intermolecular H-bond formation, occur at the same frequency of 3350 cm^{-1} (1 and 2 in Fig. 4b).

In interaction positions named as cases 3, 4 and 5 (Fig. 4c and Fig. 5a,b), only one intermolecular H-bond is formed between AdTCA and DOX. Peaks at 3314 cm^{-1} for case 3 (1 in Fig. 4c) and at 3251 cm^{-1} for case 4 (1 in Fig. 5a) corresponds to stretching vibrations of O–H bond in AdTCA, which participates in hydrogen bond formation with DOX. Let's note that peak at 2797 cm^{-1} for case 5 (1 in Fig. 5b) which corresponds to H-bond formation with nitrogen atom in DOX.

We analyze the H-bonds parameters in six cases of AdTCA–DOX molecular complex to estimate the strength of the formed H-bonds. The calculated parameters, whose analysis provides the estimation of a hydrogen bond's influence on the structure and the IR spectrum, are presented in Table 1. In the first column, the case numbers of molecular complex and H-bonds numbers are given; in the second – lengths of O–H bond in them; in the third – lengths of O–H...O and O–H...N hydrogen bridges; in the fourth – frequencies of stretching vibrations of O–H

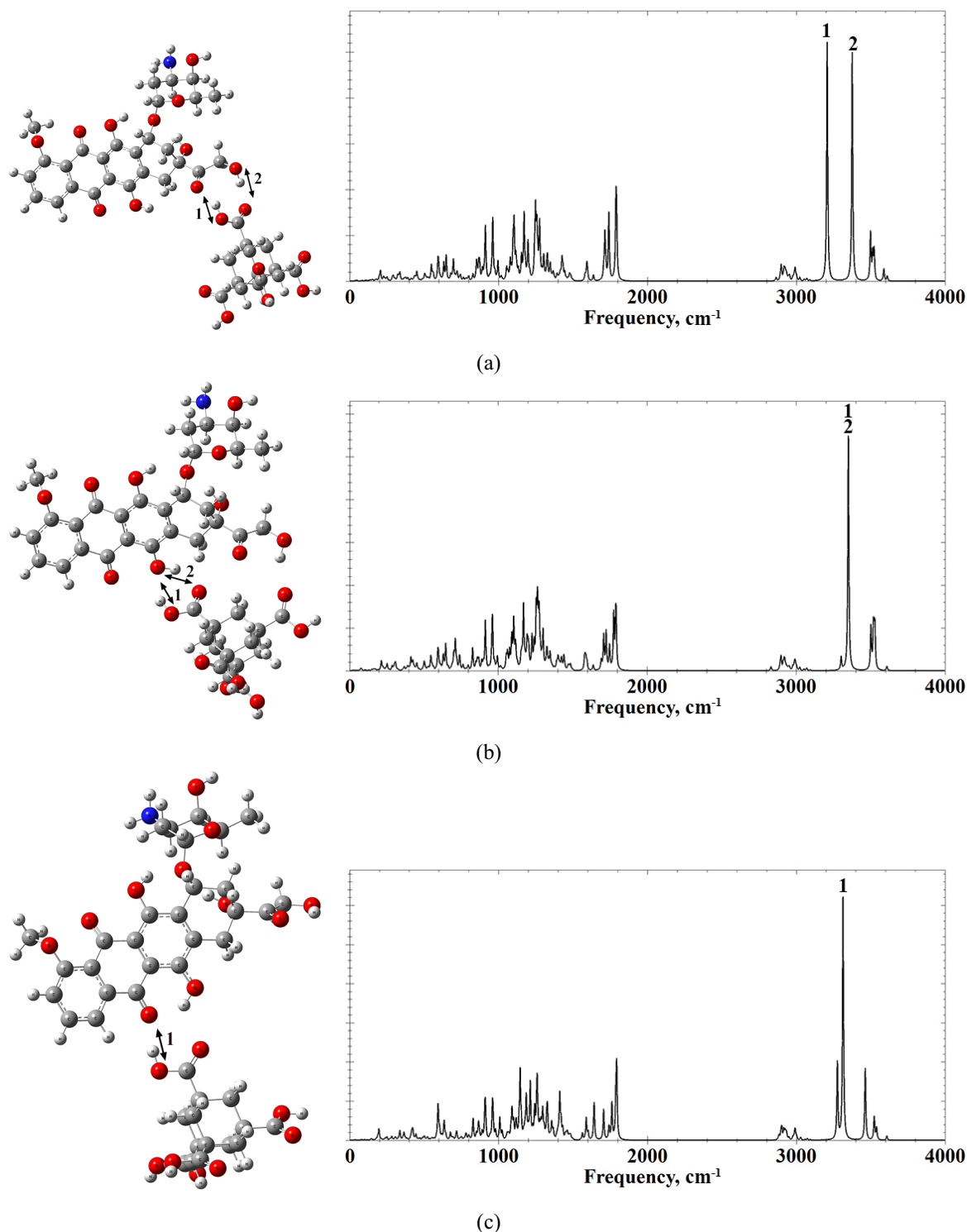


FIG. 4. Structures (left) and calculated IR spectra (right) for three cases of the molecular compound AdTCA and DOX: case 1 (a), case 2 (b), case 3 (c)

bonds; in the fifth – splitting and shifts of these frequencies in complex formation; in the sixth – formation energies of hydrogen bonds.

According to the data, presented in Table 1, it should be noted that the strongest hydrogen bond between AdTCA and DOX is formed with participation of O–H bond in AdTCA and nitrogen atom in DOX (case 5), which is expressed in the big frequency shift on 726 cm⁻¹ to the long-wavelength region. The length of the formed

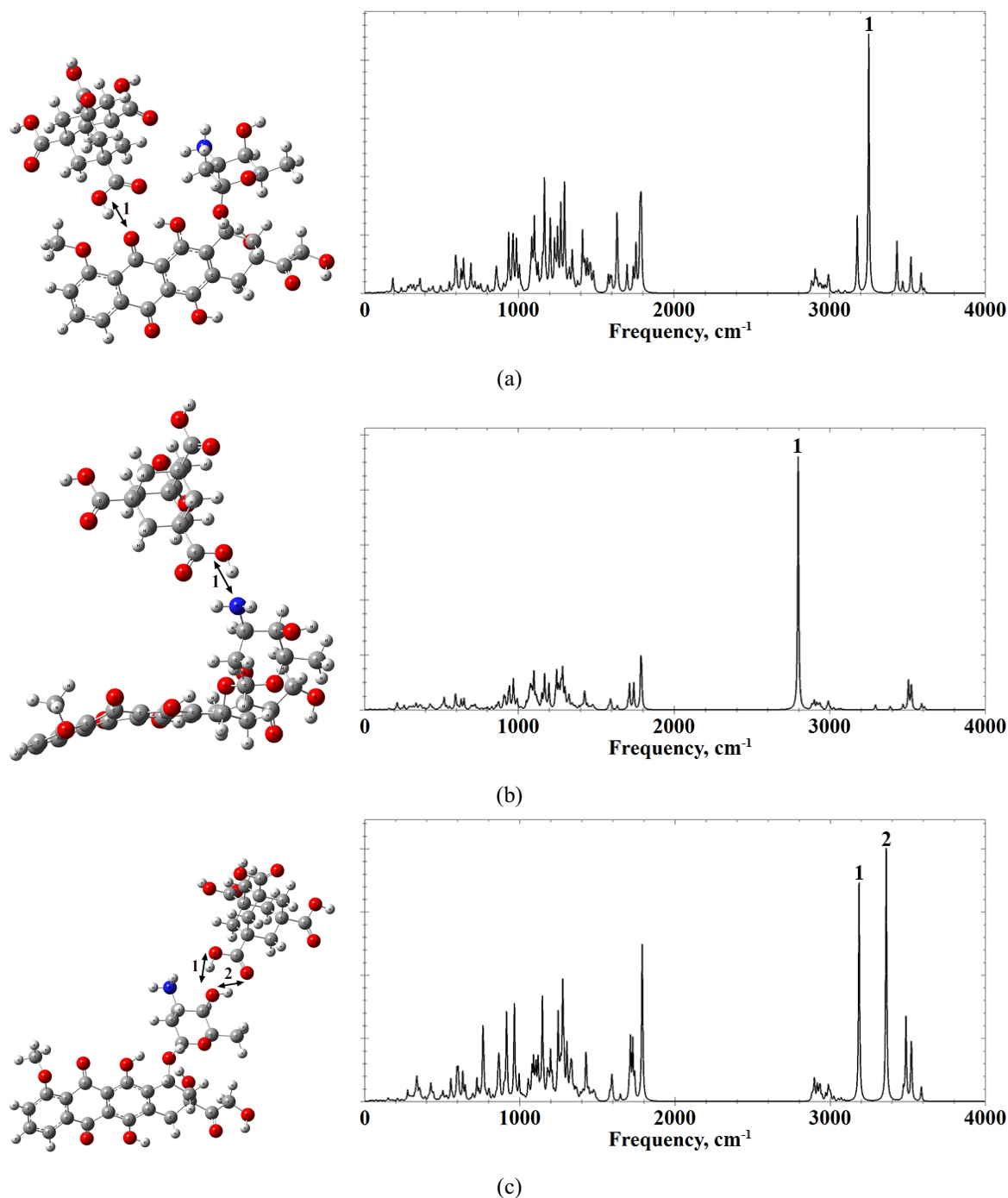


FIG. 5. Structures (left) and calculated IR spectra (right) for three cases of the molecular compound AdTCA and DOX: case 4 (a), case 5 (b), case 6 (c)

hydrogen bridge is 2.76 \AA – the shortest length among all cases of connection AdTCA–DOX. The H-bond energy is 7.857 kcal/mol , which demonstrates the existence of a strong hydrogen bond.

The hydrogen bonds for the majority of AdTCA–DOX molecular complex cases can be characterized as bonds of average force as the frequency shift for them makes size from 173 cm^{-1} in case 2 to 336 cm^{-1} in case 6 and bond energy does not exceed 5 kcal/mol . The second H-bond in case 1 can be characterized as weak bond as the frequency shift for it makes 96 cm^{-1} and the bond energy is 2.245 kcal/mol .

TABLE 1. Calculated H-bonds parameters in six cases of AdTCA–DOX molecular complexes

Case number/ bond number	OH length R_{OH} , Å	Hydrogen bridge length R_{OH-O} , Å	Frequency ν , cm^{-1}	Frequency shift $\Delta\nu$, cm^{-1}	Bond energy $-\Delta H$, kcal/mol
1/1	0.99	2.78	3207	316	4.984
1/2	0.98	2.78	3376	96	2.245
2/1	0.99	2.95	3350	173	3.46
2/2	0.98	2.8	3350	241	4.253
3/1	0.99	2.76	3314	209	3.9
4/1	0.99	2.8	3251	272	4.57
5/1	1.02	2.76 (OH–N)	2797	726	7.857
6/1	0.99	2.82	3187	336	5.161
6/2	0.98	2.86	3362	248	4.327

Thus, it is possible to note that in AdTCA–DOX molecular complex there can be seven H-bonds of average force, one strong and one weak hydrogen bond what proves existence of the rather strong electrostatic interaction between nanodiamond and DOX.

We compare our results with the experimental IR spectrum of the powder of the nanodiamond-doxorubicin complex taken from [9]. For comparison, we created the combined IR spectrum as imposing of calculated IR spectra for six cases of molecular complexes, corresponded to six interaction positions between AdTCA and DOX (Fig. 6).

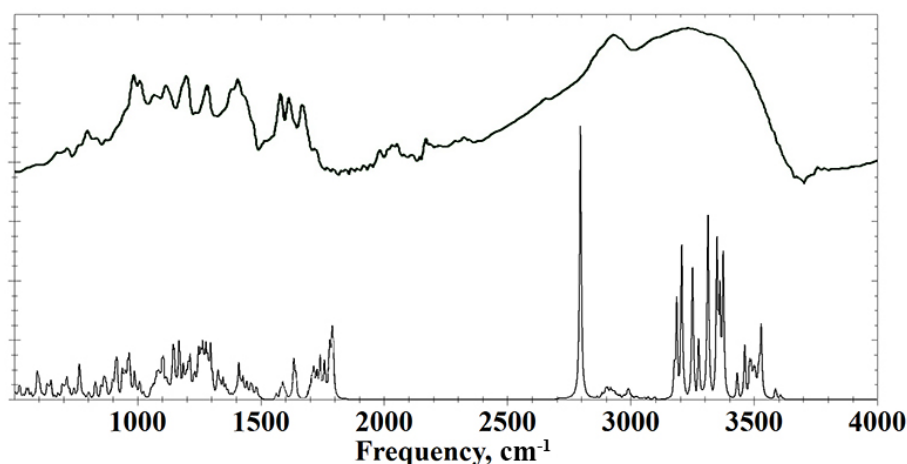


FIG. 6. Experimental IR spectrum of ND–DOX molecular complex (upper) and combined IR spectrum of six variants of AdTCA–DOX molecular complexes (lower)

As can be seen on Fig. 6, there is the good agreement of the characteristic regions in the experimental and combined IR spectra, in particular, the wide area of stretching vibrations of O–H bonds, which participate in the hydrogen bonds formation (3150 to 3600 cm^{-1}) and the peak on 2797 cm^{-1} , corresponded to stretching vibrations of O–H bond in AdTCA, which participates in hydrogen bond formation with nitrogen atom in DOX. Wide boundaries of the region, which corresponds to stretching vibrations of O–H bonds, indicate a large number of formed hydrogen bonds of various configurations in the experimental nanodiamond-doxorubicin complex, including the considered interaction variants.

4. Conclusions

During molecular modeling, it was established that AdTCA–DOX molecular complex can occur due to nine hydrogen bonds formed in six various cases for the molecular compound. One of H-bond is strong and seven

H-bonds are bonds of average force. Since the sizes of NDs, which are used in scientific experiments with DOX, are from 5 nm and higher, and the width of the DOX molecule is about 1.5 nm, it can be assumed that the DOX molecule can be attached to the ND on several points simultaneously. The combined IR spectrum, with imposing of calculated IR spectra for six cases of molecular complexes, corresponded to six interaction positions between AdTCA and DOX and was created for comparison with experimental IR spectra of ND–DOX molecular complex [9]. We can observe a good agreement between the calculated and the experimental IR spectra, especially in the high-frequency area corresponding to stretching vibrations of O–H bonds, which participate in the intermolecular hydrogen bond formation. This indicates a large number of formed hydrogen bonds in the experimental ND–DOX complex and the stability of compound as a result of electrostatic interaction.

The obtained results demonstrate that there can be strong electrostatic interaction between doxorubicin and carboxylated detonation nanodiamonds. The formed hydrogen bonds can be considered as one of main mechanisms for targeted drug delivery and for drug retention in cells and, thus, for enhancement of doxorubicin therapeutic efficacy, as observed in experiment [9].

References

- [1] *Nanotherapeutics: Drug Delivery Concepts in Nanoscience*. Ed. by Lamprecht A. CRC Press, Taylor and Francis Group, Boca Raton, 2008, 292 p.
- [2] Gupta R.B., Kompella U.B. *Nanoparticles Technology for Drug Delivery*. N.-Y. Taylor & Francis Group, 2006, 403 p.
- [3] Popova N.R., Popov A.L., Shcherbakov A.B., Ivanov V.K. Layer-by-layer capsules as smart delivery systems of CeO₂ nanoparticle based theranostic agents. *Nanosystems: physics, chemistry, mathematics*, 2017, **8** (2), P. 282–289.
- [4] Yakovlev R.Y., Solomatin A.S., et al. Detonation diamond – a perspective carrier for drug delivery systems. *Rus. J. Gen. Chem.*, 2014, **84** (2), P. 379–390.
- [5] Ho D., Wang C.-H.K., Chow E.K.-H. Nanodiamonds: The intersection of nanotechnology, drug development, and personalized medicine. *Science Advances*, 2015, **1** (7), P. 1500439.
- [6] Shenderova O.A., McGuire G.E. Science and engineering of nanodiamond particle surfaces for biological applications (Review). *Biointerphases*, 2015, **10** (3), P. 030802.
- [7] Schrand A.M., Ciftan H.S.A., Shenderova O.A. Nanodiamond particles: properties and perspectives for bioapplications. *Crit. Rev. Solid State Mater. Sci.*, 2009, **34**, P. 18–74.
- [8] Solomatin A.S., Yakovlev R.Yu., et al. Antibacterial activity of Amikacin-immobilized detonation nanodiamond. *Nanosystems: physics, chemistry, mathematics*, 2017, **8** (4), P. 531–534.
- [9] Salaam A.D., Hwang P.T.J., et al. Nanodiamonds enhance therapeutic efficacy of doxorubicin in treating metastatic hormone-refractory prostate cancer. *Nanotechnology*, 2014, **25** (42), P. 425103.
- [10] Zhang X., Hu W., et al. A comparative study of cellular uptake and cytotoxicity of multiwalled carbon nanotubes, graphene oxide, and nanodiamond. *Toxicol. Res.*, 2012, **1**, P. 62–68.
- [11] Shugalei I.V., Voznyakovskii A.P., et al. Biological activity of detonation nanodiamond and prospects in its medical and biological applications. *Russ. J. Gen. Chem.*, 2013, **83** (5), P. 851–883.
- [12] Liu K.K., Zheng W.W., et al. Covalent linkage of nanodiamondpaclitaxel for drug delivery and cancer therapy. *Nanotechnology*, 2010, **21**, P. 1–14.
- [13] Toh T.-B., Lee D.-K., et al. Nanodiamondmitoxantrone complexes enhance drug retention in chemoresistant breast cancer cells. *Mol. Pharmaceutics*, 2014, **11**, P. 2683–2691.
- [14] Plastun I.L., Agandeeva K.E., Bokarev A.N., Zenkin N.S. Diamond-like nanoparticles influence on flavonoids transport: molecular modeling. *Proc. SPIE*, 2017, 103360K.
- [15] Adnan A., Lam R., et al. Atomistic simulation and measurement of pH dependent cancer therapeutic interactions with nanodiamond carrier. *Mol. Pharmaceutics*, 2011, **8**, P. 368–374.
- [16] Petrioli R., Fiaschi A.I., et al. The role of doxorubicin and epirubicin in the treatment of patients with metastatic hormone refractory prostate cancer. *Cancer Treat. Rev.*, 2008, **34**, P. 710–8.
- [17] Saltiel E., McGuire W. Doxorubicin (adriamycin) cardiomyopathy – a critical review. *West J. Med.*, 1983, **139**, P. 332–341.
- [18] Kohn W. Nobel Lecture: Electronic structure of matterwave functions and density functionals. *Reviews of Modern Physics*, 1999, **71** (5), P. 1253–1266.
- [19] Pople J. Nobel Lecture: Quantum chemical models. *Reviews of Modern Physics*, 1999, **71** (5), P. 1267–1274.
- [20] Frisch M.J., Trucks G.W., et al. *Gaussian 09, Revision A.02*. Wallingford CT, Gaussian Inc., 2009.
- [21] Fort R.C.Jr., Schleyers P. von R. Adamantane: Consequences of diamondoid structure. *Chem. Rev.*, 1964, **64** (3) P. 277–300.
- [22] Ermer . Five-fold diamond structure of adamantane-1,3,5,7-tetracarboxylic acid. *Journal of American Chemical Society*, 1988, **110** (12), P. 3747–3754.
- [23] Iogansen A.V. *IR Spectroscopy and Hydrogen Bond Energy Determination*. Hydrogen Bond, Nauka, Moscow, 1981, P. 112–155 (in Russian).